Junchao Zhou
Ao Chen
Yihan Liu
Jianjie Gao ✉
Jie Zhang
Haiping Du
Fei Tang

https://doi.org/10.21278/TOF.493069424
ISSN 1333-1124
eISSN 1849-1391

A MULTI-OBJECTIVE FUZZY ROBUSTNESS OPTIMISATION METHOD FOR THE SUSPENSION PARAMETERS OF A STRADDLE-TYPE MONORAIL VEHICLE

Summary

The dynamic performance of a single axle bogie straddle-type monorail vehicle (STMV) includes safe operation and lateral stability. Sensitivity analysis is used to creatively propose a multi-objective fuzzy robust optimisation (MOFRO) method aimed at improving its lateral stability under unpredictable factors. The key suspension parameters were determined through sensitivity analysis based on orthogonal experiments. The fuzzy set method transforms multi-objective functions into single objective optimisation to find the global optimal solution. The results show that the proposed strategy improves the lateral stability of the vehicle under dynamic operating conditions, significantly reducing yaw acceleration RMS, lateral acceleration RMS, and overturning the coefficient by 8.3%, 5.4%, and 26.8%. This method provides a new framework for optimising suspension design and addresses the challenge of lateral stability under dynamic conditions.

Key words: *straddle-type monorail vehicle; suspension parameters; multi-objective fuzzy robust optimisation; sensitivity analysis; lateral stability*

1. Introduction

Urban rail transit is one of the most frequently used modes of transportation primarily due to constant traffic jams and air pollution [1]. The advantages of new STMVs with single-axle bogies, a special running mechanism of urban rail transportation systems, include low noise, low cost, great climbing ability, and reduced land occupation. In China, it is becoming a significant mode of transportation for city dwellers [2]. Accordingly, specifications are presented for increased comfort, safety, and stability. These specifications include lateral stability, which is crucial for the dynamic performance of the car. The vehicle's mismatched dynamic properties and unstable single-axle bogie structure impact its lateral stability. Vehicles also have to deal with many unknowns, such as shifting loads and speeds.

Dynamic modelling has been used extensively in recent years to study the lateral stability of STMVs with single-axle bogies [3]. Two different models of articulated monorail vehicles have been set up, and their dynamic properties after passing the bend studied. Wang and Zhu [4] investigated the effects of skidding on vehicle acceleration and ride comfort and calculated the equations of motion that govern the monorail train-bridge interactive system. Xu and Lu [5] developed a coupled dynamic model of the STMV system and investigated its vibration stability and operational safety in various spatial configurations. Multi-body dynamics and finite element modelling techniques were employed to construct a vehicle-rail spatially coupled dynamics model and evaluate the dynamics of the monorail-bridge system [6,7]. Maciel and Barbosa [8] developed the vehicle's mathematical model and investigated how stability affected the dynamic response. Additionally, various scientists have conducted research on the mechanism of lateral stability. Their findings indicate that the vehicle centrifugal force, which prevents the line of action for vehicle loads from passing through the centroid of the track beam's section and causes the track beam to twist, gives rise to the head-shaking that occurs when the monorail vehicle negotiates a curve. These findings led to the proposal of a method for shimmy analysis of the vehicle using the factor model [9-11]. Furthermore, bifurcation theory was applied to investigate the hunting stability of the vehicle [12,13]. Despite these advances, the main issue in researching the lateral stability of STMVs with single-axle bogies lies in how to make the vehicle more stable.

Consequently, researchers have worked hard to improve the lateral stability of STMV single-axle bogies. Control methods are used to maintain vehicle stability and improve ride comfort [14,15], such as magnetorheological control [16], predictive performance control [17] and decoupling vibration control [18]. Many scholars have suggested clever techniques to address optimisation issues [19,20]. The vehicle's design parameters have been tuned to enhance both its running quality and lateral stability [21,22]. The vehicle's suspension characteristics were optimised using a genetic algorithm, leading to an increase in ride comfort and a decrease in the overturning coefficient [23,24]. Wen, Huang [25] optimised the structural and dynamic parameters to increase the comfort of the vehicle with an improved genetic algorithm. Wu, Du [26] optimised the steering torque of each wheel system with an NSGA-II algorithm to improve the cornering performance of the vehicle. Unfortunately, the research mentioned above primarily concentrates on optimising vehicle characteristics under a single operating state, ignoring the impact of modifications to vehicle operating conditions, such as load and speed. Sub-objectives in the optimisation process may clash, meaning that improving one sub-objective could negatively impact the performance of one or more other sub-objectives.

Given these issues, this study uses the sensitivity analysis method to identify the suspension factors that have a major impact on lateral stability. By using a fuzzy set and considering the influence of uncertain factors, a MOFRO method is innovatively proposed to optimise the suspension parameters and enhance the vehicle’s lateral stability. This strategy provides fresh insights and techniques for improving the rubber-type vehicle design.

This paper's primary innovations and contributions are as follows:

(1) A sensitivity analysis method based on multifactorial and multilevel orthogonal experiments to obtain the key influential parameters to achieve a reduction in the number of suspended parameters in the optimisation problem.

(2) A new fuzzy set to express each optimisation objective as a membership function to enable measurement within the same dimension. Ultimately, the problem is converted from a multi-objective robust problem to a single-objective one.

(3) A MOFRO model of suspension parameters for the vehicle.

The remainder of the article is structured as follows. To determine the suspension parameters that are crucial for the vehicle's lateral stability, Section 2 employs a sensitivity

analysis method based on multi-factor and multi-level orthogonal tests. In Section 3, a MOFRO model of suspension parameters is suggested to enhance the vehicle's lateral stability. The optimisation findings are examined and discussed in Section 4. Finally, conclusions are given in Section 5.

2. Sensitivity analysis of suspension parameters of STMVs with single-axle bogies

2.1 Dynamic model of STMVs with single-axle bogies

Figure 1 shows that the dynamic model is required to increase the lateral stability of an STMV with single-axle bogies. The body of the vehicle and bogies make up the STMV with single-axle bogies. There are three types of wheels on each bogie: steering, running, and stabilising. A suspension system of transverse dampers, vertical dampers, air springs and transverse stops connects the vehicle body to the bogie.

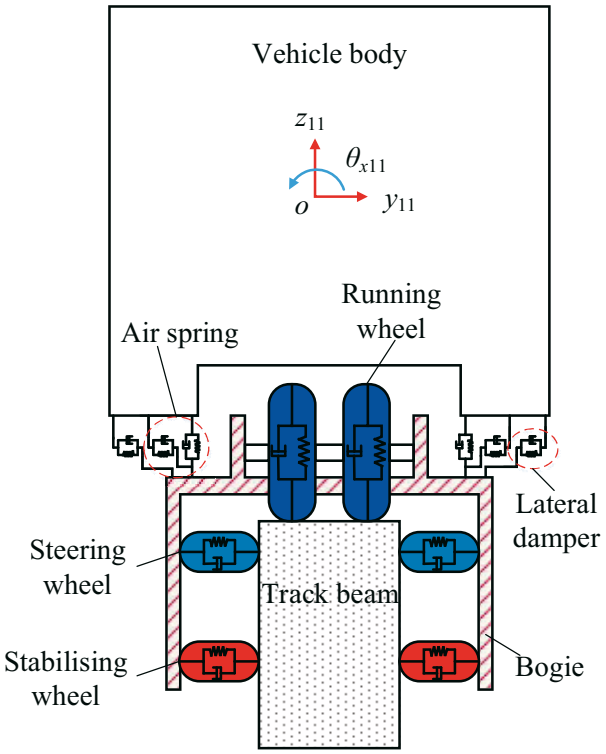

(a)

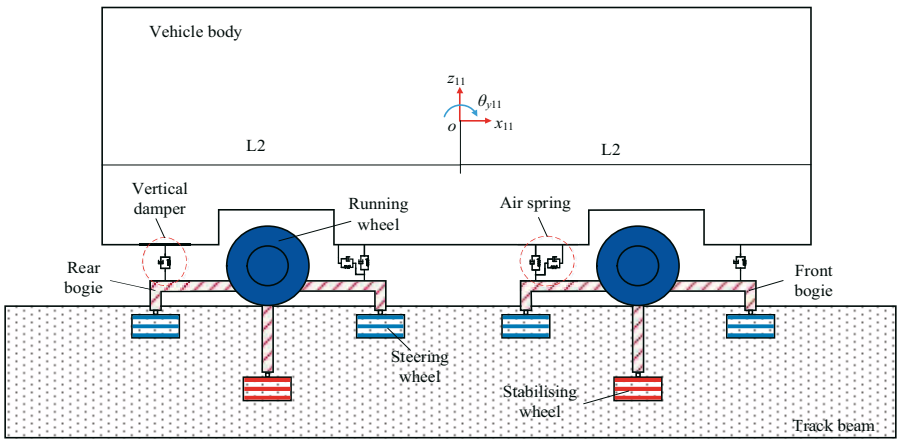

(b)

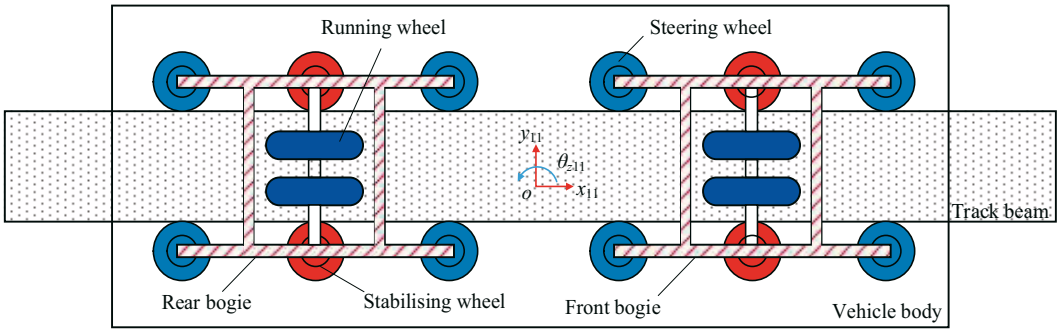

(c)

Fig. 1 Dynamic model of an STMV with single-axle bogies. (a) Left view, (b) Main view, (c) Top view.

By considering the vehicle and bogie roll, the vertical, lateral, pitch and yaw motions, Equation (1) is derived from the Lagrange equation:

$$\frac{\mathrm{d}}{\mathrm{d}t}\left(\frac{\partial T}{\partial \dot{q}_j}\right)-\frac{\partial T}{\partial q_j}+\frac{\partial U}{\partial q_j}+\frac{\partial W}{\partial \dot{q}_j}=Q_j \tag{1}$$

where T, U, W, Q_j, q_j are kinetic energy, potential energy, damping dissipation, generalised force and torque, and generalised coordinates, respectively. Among them, the expressions for kinetic energy, potential energy, and damping energy dissipation can be found in:

$$T=\frac{1}{2}\left(\begin{matrix}\mathrm{m}_{11}\dot{\mathrm{x}}_{11}{}^2+\mathrm{m}_{11}\dot{\mathrm{y}}_{11}{}^2+\mathrm{m}_{11}\dot{\mathrm{z}}_{11}{}^2+\\ \mathrm{I}_{\mathrm{x}11}\dot{\theta}_{\mathrm{x}11}{}^2+\mathrm{I}_{\mathrm{y}11}\dot{\theta}_{\mathrm{y}11}{}^2+\mathrm{I}_{\mathrm{z}11}\dot{\theta}_{\mathrm{z}11}{}^2\end{matrix}\right)+\frac{1}{2}\sum_{i=1}^{2}\left(\begin{matrix}\mathrm{m}_{2\mathrm{i}}\dot{\mathrm{x}}_{2\mathrm{i}}{}^2+\mathrm{m}_{2\mathrm{i}}\dot{\mathrm{y}}_{2\mathrm{i}}{}^2+\mathrm{m}_{2\mathrm{i}}\dot{\mathrm{z}}_{11}{}^2+\\ \mathrm{I}_{\mathrm{x}2\mathrm{i}}\dot{\theta}_{\mathrm{x}2\mathrm{i}}{}^2+\mathrm{I}_{\mathrm{y}2\mathrm{i}}\dot{\theta}_{\mathrm{y}2\mathrm{i}}{}^2+\mathrm{I}_{\mathrm{z}2\mathrm{i}}\dot{\theta}_{\mathrm{z}2\mathrm{i}}{}^2\end{matrix}\right) \tag{2}$$

$$U=\frac{1}{2}\sum_{i=1}^{2}\sum_{j=1}^{2}\sum_{n=1}^{2}\left(\begin{matrix}K_{1ijn}R_{1ijn}{}^2\delta_{1j}+K_{2ijn}R_{2ijn}{}^2+K_{3ijn}R_{3ijn}{}^2\\ +K_{4ijn}R_{4ijn}{}^2\delta_{4j}+K_{5ijn}R_{5ijn}{}^2\delta_{5j}\end{matrix}\right) \tag{3}$$

$$W=\frac{1}{2}\sum_{i=1}^{2}\sum_{j=1}^{2}\sum_{n=1}^{2}\left(\begin{matrix}C_{1ijn}\dot{R}_{1ijn}{}^2\delta_{1j}+C_{2ijn}\dot{R}_{2ijn}{}^2+C_{3ijn}\dot{R}_{3ijn}{}^2\\ +C_{4ijn}\dot{R}_{4ijn}{}^2\delta_{4j}+C_{5ijn}\dot{R}_{5ijn}{}^2\delta_{5j}\end{matrix}\right) \tag{4}$$

In the following equations, m_{11} and m_{2i} are the mass of the vehicle body and bogie, respectively. $\dot{x}$, $\dot{y}$, $\dot{z}$, $\dot{\theta}$ are the longitudinal velocity, lateral velocity, vertical velocity and angular velocity, respectively. I is the rotational inertia. K_{1ijn}, C_{1ijn} are the vertical rigidity and vertical damping of the air spring, K_{2ijn}, C_{2ijn} are the rigidity and damping of the running wheel, K_{3ijn}, C_{3ijn} are the rigidity and damping of the steering wheel, K_{4ijn}, C_{4ijn} are the rigidity and damping of the stabilising wheel, and K_{5ijn}, C_{5ijn} are the lateral rigidity and lateral damping of the air spring. $R_{rijn}(r=1,2,3,4,5)$ is the relative displacement of the air spring and damper, i is the bogie position ($i=1,2$ represent the front and rear bogies), j is the longitudinal position of the tyre in the bogie ($j=1,2$ represent the front and rear tyres), n is the lateral position of the tyre in the bogie ($n=1,2$ denote the left and right tyres), and δ_{rj} is the Kronecker function $(r=1,2,3,4,5)$. The main suspension parameters of the single-axle bogie straddle-type monorail vehicle are shown in Table 1. This article ignores the damping of the air springs.

Table 1 Main suspension parameters of an STMV with a single-axle bogie.

Parameters	Values	Unit
Torque shaft length (L)	0.587	m
Drawbar length ($L1$)	0.83	m
Half distance of vehicle ($L2$)	4.56	m

Vertical of air spring rigidity (K_{1ijn})	510000	N/m
Vertical of air spring damping (C_{1ijn})	45400	Ns/m
Vertical rigidity of running wheel (K_{2ijn})	1400000	N/m
Cornering rigidity of running wheel (K_{2yijn})	158380	N/m
Vertical rigidity of steering wheel (K_{3ijn})	530000	N/m
Vertical rigidity of stabilising wheel (K_{4ijn})	980000	N/m
Lateral of air spring rigidity (K_{5ijn})	950000	N/m
Lateral of air spring damping (C_{5ijn})	1000	Ns/m
Longitudinal of air spring rigidity (K_{6ijn})	950000	N/m
Longitudinal of air spring damping (C_{6ijn})	1000	Ns/m
Rigidity of lateral damper (K_y)	510000	N/m
Damping of lateral damper (C_y)	15000	Ns/m
Rigidity of vertical damper (K_z)	510000	N/m
Damping of vertical damper (C_z)	35000	Ns/m

2.2 Sensitivity analysis of the suspension parameters based on multi-factor and multi-level orthogonal experiments

The multitude of suspension characteristics means that each one affects the vehicle lateral stability in a unique way. The optimisation objectives (yaw acceleration RMS, lateral acceleration RMS, and the overturning coefficient) are used as the evaluation indexes of the vehicle lateral stability to lessen the blindness of the optimal design of the suspension parameters. Sensitivity analyses were conducted using multifactorial and multistage orthogonal experimental methods based on the dynamic model of an STMV with single-axle bogies [27].

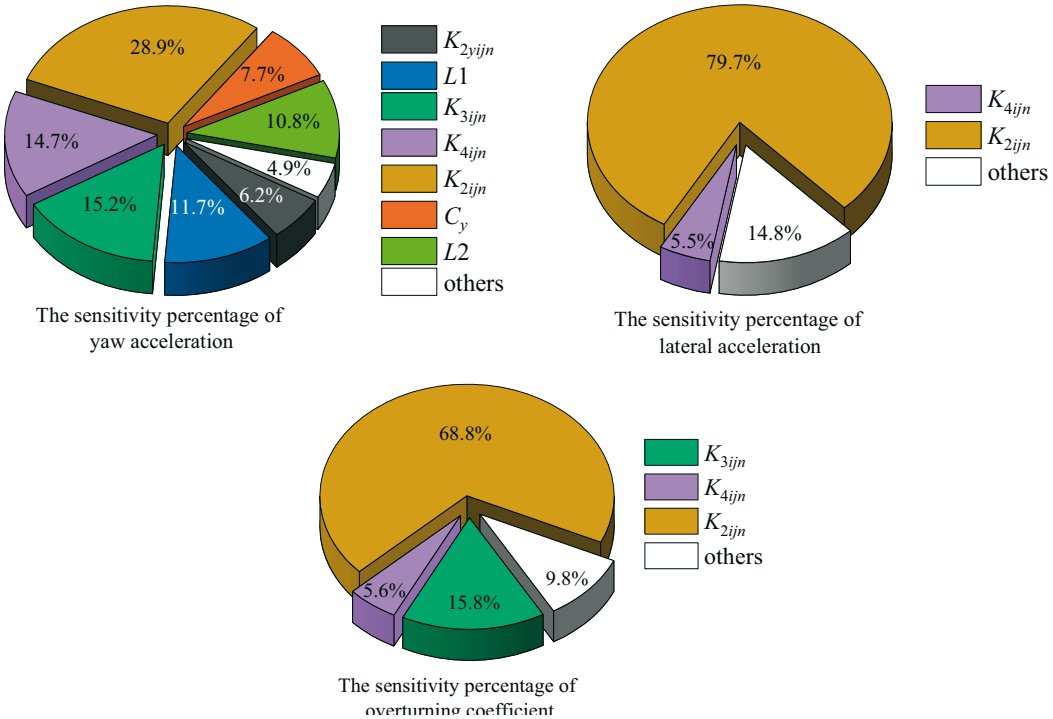

Fig. 2 Parameter sensitivity analysis results.

The multi-factor and multi-level orthogonal experimental method was used to investigate the sensitivity of the suspension parameters. Figure 2 explains the sensitivity relationship between the suspension parameters and the lateral stability optimisation objective.

With a sensitivity percentage greater than 5%, the parameters that affect the output index can be observed. The following conclusions are drawn from Figure 2:

(1) The following characteristics significantly affect the yaw acceleration: running wheel vertical rigidity, steering wheel vertical rigidity, stabilising wheel vertical rigidity, drawbar length, vehicle half distance, lateral damper damping, running wheel cornering rigidity.

(2) The vertical rigidity of the running wheel is greater than the vertical rigidity of the stabilising wheel, and these factors have a significant impact on lateral acceleration.

(3) The following parameters, in order of significant to minor impact on the overturning coefficient, are listed: running wheel vertical rigidity comes before the steering wheel and stabilising wheel vertical rigidity.

Thus, the following primary factors can be eliminated to reduce the impact on the lateral stability of an STMV with single-axle bogies: drawbar length, vehicle half distance, running wheel vertical rigidity, running wheel cornering rigidity, steering wheel vertical rigidity, stabilising wheel vertical rigidity, and lateral damper damping.

3. A MOFRO model of suspension parameters for an STMV with single-axle bogies

3.1 The MOFRO method

A methodology to obtain the design parameters and optimal solutions with higher reliability and robustness is the objective of the robust optimisation method. This approach takes into consideration the influence of design parameter fluctuations on the optimisation objectives and aims to reduce the target sensitivity response to the design parameters. In engineering applications, the multi-objective robust optimisation problem can be formulated as follows [28]:

$$\begin{cases} \min \quad F_k(x) = F[\mu_k(x), \sigma_k(x)] & k = 1, 2, ..., m \\ s.t. \quad \mathrm{G}_i(x) = \mu_{G_i(x)} + n\sigma_{G_i(x)} \le C & i = 1, 2, ..., q \\ \qquad x_{jL} + n\sigma_{x_j} < \mu_{x_j} < x_{jU} - n\sigma_{x_j} & j = 1, 2, ..., p \end{cases} \tag{5}$$

where $F_k(x)$ is the k_{th} sub-objective function, and m is the number of sub-objective functions. $\mu_k(x)$ and $\sigma_k(x)$ are the mean value and mean square deviation of the optimisation function, respectively. $\mathrm{G}_i(x)$ is the i_{th} constraint condition. $\mu_{G_i(x)}$ and $\sigma_{G_i(x)}$ are the mean value and mean square deviation of the i_{th} constraint condition, respectively. C is the constraint value, and q is the number of constraints. μ_{x_j} and σ_{x_j} are the mean value and mean square deviation of the j_{th} design variable, respectively. x_{jL} and x_{jU} are the lower and upper limits of the j_{th} design variable, respectively. p is the number of design variables, and n is the quality level of the σ constraint. The change of n value can change the optimisation quality.

In the multi-objective optimal problem described in Equation (5), the sub-objectives exhibit mutual constraints and differ in terms of dimensions and ranges [29]. To simplify the multi-objective optimal problem, a fuzzy set is employed. Each optimisation objective is represented by a membership function, which allows for evaluating the objectives in the same

dimension [30]. The exact type of member function is determined empirically. For the multi-objective optimal problem, the parabolic membership function is found to be more suitable [31]. The corresponding form of the membership function is as follows:

$$P_k(x)=\begin{cases}0 & F_k(x)<F_{ka}\\ \left(\dfrac{F_k(x)-F_{ka}}{F_{kb}-F_{ka}}\right)^s & F_{ka}\le F_k(x)\le F_{kb}\\ 1 & F_k(x)>F_{kb}\end{cases} \tag{6}$$

where s is the index of the membership function and $s=1$ or 2 represent linear or quadratic membership functions, respectively [32]. Due to the fact that the multi-objective optimal problem is highly non-linear, the quadratic membership function is used here. F_{kb} and F_{ka} are the maximum and minimum values of the function $F_k(x)$ in the k_{th} sub-objective optimisation process, respectively. The value of each optimisation objective, as represented by the corresponding membership function, varies from 0 to 1. Therefore, each optimisation objective can be measured in the same dimension.

The weight coefficient is adopted to combine the membership functions. Thus, the multi-objective optimal problem is converted into a single-objective problem:

$$D(x)=\sum_{k=1}^{m} w_k P_k(x), k=1,2,...,m \tag{7}$$

where w_k is the weight coefficient of the k_{th} sub-objective function $F_k(x)$. It is assumed that each objective function is equally optimised:

$$w_1+w_2+...+w_m=1 \tag{8}$$

$$w_1=w_2=...=w_m \tag{9}$$

According to Equations (5)-(9), an MOFRO mathematical model can be established:

$$\begin{cases}\min \quad D(x)=\sum_{k=1}^{m} w_k P_k(x) & k=1,2,...,m\\ s.t. \quad \mathrm{G}_i(x)=\mu_{G_i(x)}+n\sigma_{G_i(x)}\le C & i=1,2,...,q\\ \qquad x_{jL}+n\sigma_{x_j}<\mu_{x_j}<x_{jU}-n\sigma_{x_j} & j=1,2,...,p\end{cases} \tag{10}$$

3.2 Optimisation objectives

In the MOFRO mathematical model, the evaluation indices for vehicle lateral stability are the yaw acceleration RMS, lateral acceleration RMS, and the overturning coefficient. The optimisation objectives can be represented as follows:

$$F_1(x)=\left[\frac{1}{N}\sum_{i=1}^{N}\left[\ddot{\theta}_{z11}(i)\right]^2\right]^{\frac{1}{2}} \tag{11}$$

$$F_2(x)=\left[\frac{1}{N}\sum_{i=1}^{N}\left[\ddot{y}_{11}(i)\right]^2\right]^{\frac{1}{2}} \tag{12}$$

$$F_3(x)=D=\frac{P_d}{P_{st}}=\frac{P_2-P_1}{P_2+P_1} \tag{13}$$

Among them, $F_1(x)$, $F_2(x)$, $F_3(x)$ represent the yaw acceleration RMS, the lateral acceleration RMS, and the overturning coefficient, respectively. N denotes the number of sample points of the sampling points. $\ddot{\theta}_{z11}$(i) represents the yaw acceleration value of the i_{th} sample point, $\ddot{y}_{11}$(i) represents the lateral acceleration value of the i_{th} sample point, P_d is the difference between the vertical loads of the left and right running wheels, and P_{st} is the sum of the vertical loads of the left and right running wheels. P_2, P_1 are the vertical load of the running wheel on the side of loading and unloading, respectively.

3.3 Selection of design parameters

Design parameters in robust optimisation can be divided into two categories: noisy factors and controlled elements. The following parameters are identified as controllable factors that the designer can determine: vertical rigidity of the running wheel, the half distance of the vehicle, drawbar length, cornering rigidity of the running wheel, vertical rigidity of the steering wheel, vertical rigidity of the stabilising wheel, and damping of the lateral damper. This is based on the sensitivity analysis of the design parameters for an STMV with single-axle bogies in Section 2.

Table 2 Design parameters and value range.

Design parameters	Design variables	Parameters	Lower limit	Upper limit	Unit
Controllable factors $(x_1 \sim x_7)$	x_1	$L1$	0.33	1.33	m
	x_2	$L2$	4.46	4.66	m
	x_3	K_{2ijn}	980000	1820000	N/m
	x_4	K_{2yijn}	110866	205894	N/m
	x_5	K_{3ijn}	265000	795000	N/m
	x_6	K_{4ijn}	490000	1470000	N/m
	x_7	C_y	7500	22500	Ns/m
Noise factors (x_8, x_9)	x_8	M	10793	21893	kg
	x_9	v	20	40	m/s

During the operation of the vehicle, variations in load and speed cause changes in the vehicle lateral stability. As a result, load (M) and speed (v) are selected as noise factors, which are not directly under the control of the designer. The range of the design parameters is presented in Table 2.

3.4 Constraint condition

Due to the special structural characteristics of an STMV with single-axle bogies, its running mechanism is unique. The stability, comfort, and safety of the vehicle are affected by

vehicle dynamics. This paper refers to the current research on the vehicle and the relevant evaluation standards for railway vehicles. The optimisation process considers three key indexes: operational stability, stability, and curve negotiation ability. These indexes are treated as constraint conditions during the optimisation process to ensure the desired levels of stability, comfort, and safety.

(1) Wheel load reduction rate

Operational stability and cornering pass ability are assessed by the rate of wheel load reduction (which is the load difference between the inner and outer wheel). The mathematical expression for it is:

$$\frac{\Delta P}{P} = \frac{P_2 - P_1}{P_2 + P_1} \tag{14}$$

where P_1 and P_2 are the vertical force of the wheel on the load-reducing side and the vertical force of the wheel on the load-increasing side. According to the vehicle standard test specification, the rate of wheel load reduction is $\Delta P / P \leq 0.6$.

(2) The roll angle of the vehicle body

The roll angle has significant implications for both the curve negotiation ability and the overall stability of the vehicle, as well as the comfort of passengers. Extensive research conducted by the Japanese Monorail Association has revealed that the roll angle of the vehicle body (θ) should be kept within an acceptable range to satisfy safety and comfort requirements. Specifically, it is recommended to ensure that the roll angle remains below 10°, expressed as [33]:

$$\theta < 10° \tag{15}$$

(3) The steering torque

When the vehicle passes through a curve, the radial force of the steering wheel and the steering torque of the bogie change. To prevent the excessive influence of curve negotiation during the optimisation process, it is advisable to keep the optimised steering torque within reasonable limits and for it not to be too large [33]:

$$M_d \leq 1.4 M_0 \tag{16}$$

where M_d is the steering torque when the vehicle is running, and M_0 is the initial steering torque.

(4) The RMS value of total weighted acceleration

The evaluation of human vibration by ISO 2631 [34] can be used as an evaluation index of stability for vehicle operations. Considering the three directions (lateral, vertical, and longitudinal), the acceleration time domain curves are measured. These curves are then transformed to obtain frequency spectrum curves. Finally, the power spectral density function $G_a(f)$ is obtained by spectrum analysis. The RMS value of the weighted acceleration $a_{\omega i}$ $(i = x, y, z)$ is calculated by Equation (17):

$$a_{\omega i} = \sqrt{\int_{0.5}^{80} \omega^2(f) G_a(f) \mathrm{d}f} \tag{17}$$

where $\omega(f)$ and $G_a(f)$ is the frequency-weighted function and the power spectral density function. The RMS values of acceleration in the lateral, vertical, and longitudinal directions are determined by Equation (18) to obtain the RMS value of total weighted acceleration:

$$a_\omega = \sqrt{(1.4a_{\omega x})^2 + (1.4a_{\omega y})^2 + a_{\omega z}^2} \tag{18}$$

According to the relationship between a_ω and human ride comfort in ISO 2631, there is a limit set at $a_\omega < 0.315\text{m/s}^2$.

3.5 The MOFRO model of suspension parameters

Using the goal components outlined in the specified objectives, the multi-objective optimisation of suspension parameters is the main emphasis of this study [35]. The optimisation is carried out using the MOFRO method, with the following mathematical model representing the procedure:

$$\begin{cases} \min \quad D(x) = \sum_{k=1}^{m} w_k P_k(x) & k = 1,2,3 \\ s.t. \quad \mu_{G_1(x)} + 6\sigma_{G_1(x)} \le 0.6 \\ \qquad \mu_{G_2(x)} + 6\sigma_{G_2(x)} \le 10 \\ \qquad \mu_{G_3(x)} + 6\sigma_{G_3(x)} \le 1.4M_0 \\ \qquad \mu_{G_4(x)} + 6\sigma_{G_4(x)} \le 0.315 \\ \qquad x_{jL} + 6\sigma_{x_j} < \mu_{x_j} < x_{jU} - 6\sigma_{x_j} & j = 1,2,...,9 \end{cases} \tag{19}$$

where $G_1(x)$, $G_2(x)$, $G_3(x)$ and $G_4(x)$ are the rate of wheel load reduction, roll angle of the vehicle body, steering torque and the RMS value of total weighted acceleration, respectively. x_j are the design parameters. The weight coefficient is $w_1 = w_2 = w_3 = 1/3$, $P_1(x)$ is the membership function for the RMS of yaw acceleration, $P_2(x)$ is the membership function for the RMS of lateral acceleration, and $P_3(x)$ is the membership function for the overturning coefficient. It can be expressed as:

$$P_j(x) = \left(\frac{F_j(x) - F_{ja}}{F_{jb} - F_{ja}} \right)^2, \; j = 1,2,3 \tag{20}$$

$F_k(x) = F[\mu_k(x), \sigma_k(x)] = \lambda \mu_k{}^2(x) + (1-\lambda)\sigma_k{}^2(x)$ is the objective function of robust optimisation, where $k = 1,2,3$. λ is a weighting factor, and $\lambda = 0.5$. F_{1a} and F_{1b} represent the maximum and minimum values of the function $F_1(x)$ in the optimisation process, respectively. F_{2a} and F_{2b} represent the maximum and minimum values of the function $F_2(x)$ in the optimisation process, respectively, while F_{3a} and F_{3b} represent the maximum and minimum values of the function $F_3(x)$, respectively.

4. The MOFRO of suspension parameters

4.1 The optimisation process

The NSGA-II optimisation technique is used to solve the objective functions within the range of vehicle design parameters based on the MOFRO model and the vehicle dynamics model. To find the parameter combination for MOFRO, iterative optimisation is performed using the optimisation convergence criterion. Table 3 contains a list of the optimisation algorithm's parameters. The vehicle dynamics model and the Monte Carlo analysis principle are used to analyse the optimisation outcomes produced. Figure 3 depicts the particular MOFRO optimisation procedure.

Table 3 The parameter setting of the optimisation algorithm.

Population size	Number of generations	Crossover probability	Mutation probability
30	20	0.8	0.3

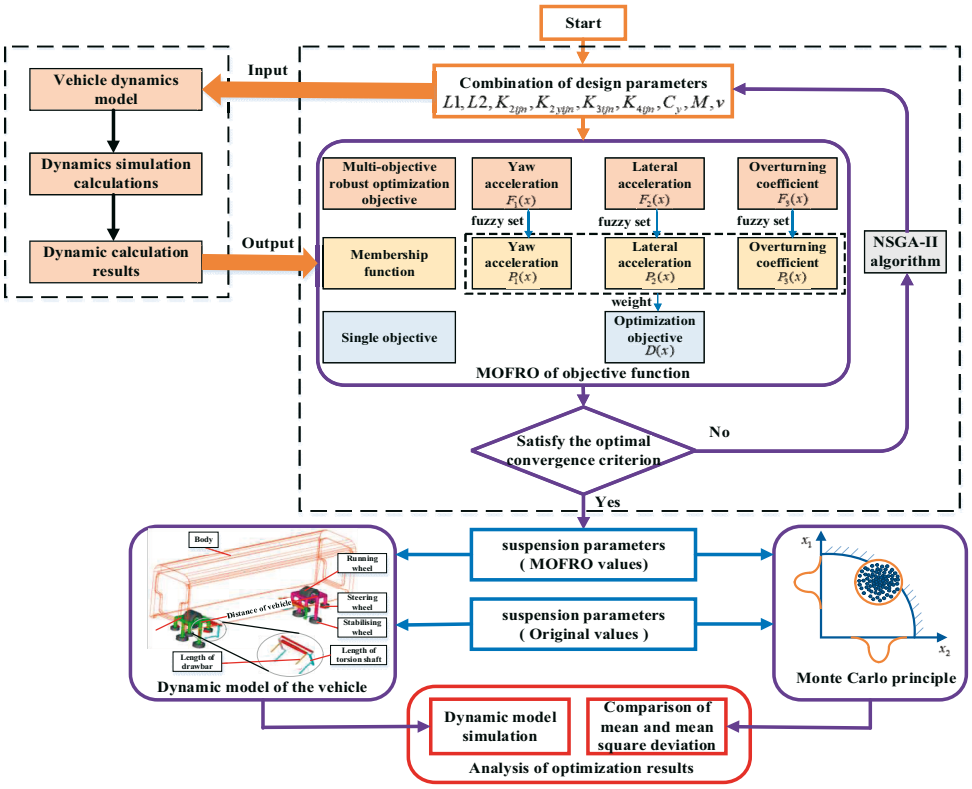

Fig. 3 MOFRO process of suspension parameters of the vehicle.

4.2 Optimisation results and discussion

According to the MOFRO model and optimisation process in Section 4, the MOFRO is used to optimise the suspension parameters of the vehicle. The iterative optimisation calculation persists until convergence is achieved or the maximum generation limit is reached. The parameters of the vehicle converge after nearly 600 iterations, as indicated in Figure 4. Furthermore, the average value of the optimisation objective in Figure 5 is approximately 0.00001 to achieve convergence.

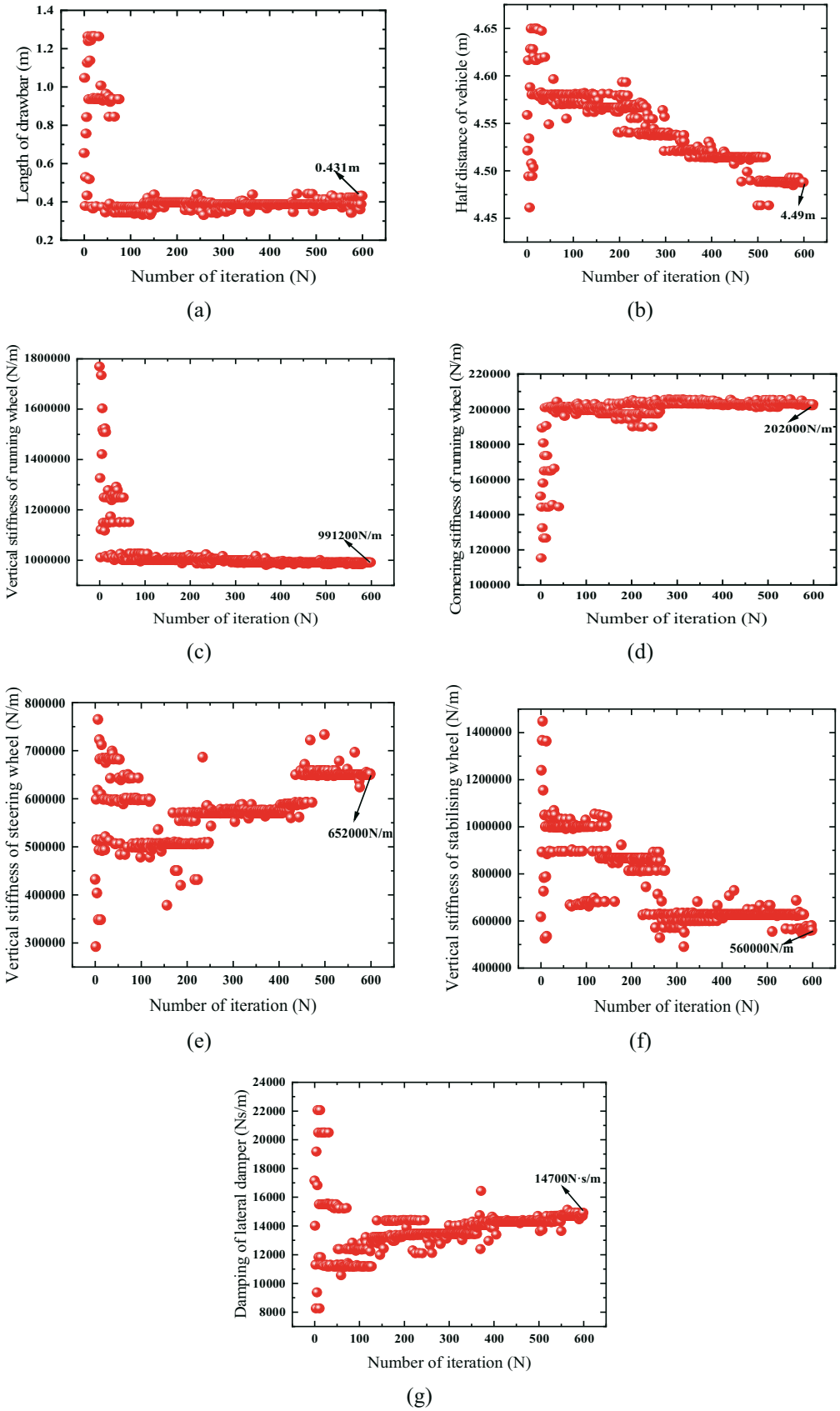

Fig. 4 The iterative optimisation process of the suspension parameters for the vehicle: (a) drawbar length; (b) half distance of vehicle; (c) vertical stiffness of running wheel; (d) cornering stiffness of running wheel; (e) vertical stiffness of steering wheel; (f) vertical stiffness of stabilising wheel; (g) damping of lateral damper.

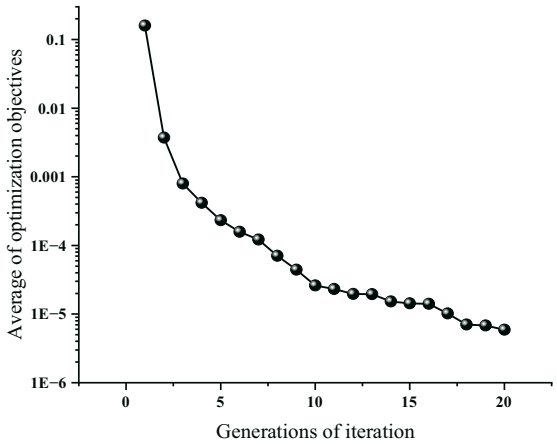

Fig. 5 The iterative optimisation process of the optimisation objective.

Using the MOFRO approach reduces the yaw acceleration RMS, the lateral acceleration RMS, and the overturning coefficient by 8.3%, 5.4%, and 26.8%, respectively. The goal of properly reducing the objective functions is accomplished, enhancing the vehicle's lateral stability. Table 4 presents the outcomes of the vehicle's optimisation.

Table 4 The results of the optimization.

Optimisation objectives and parameters	Name	Original scheme	MOFRO	Optimisation rate
Design parameter	$L1$	0.83	0.431	-48.1%
	$L2$	4.56	4.49	-1.5%
	K_{2ijn}	1400000	991200	-30.2%
	K_{2yijn}	158380	202000	+27.5%
	K_{3ijn}	530000	652000	+23%
	K_{4ijn}	980000	560000	-42.9%
	C_y	15000	14700	-2%
Optimisation objective	$F_1(x)$	1.21	1.11	-8.3%
	$F_2(x)$	0.351	0.332	-5.4%
	$F_3(x)$	0.239	0.175	-26.8%

4.2.1 Monte Carlo analysis of optimisation results

To analyse the robustness of the optimisation results, the Monte Carlo analysis principle is implemented (sampling and calculation performed 1000 times). The aim is to evaluate whether the optimised results exhibit improved robustness. It is clear from Table 5 that the mean value and mean square deviation for the yaw acceleration RMS, the lateral acceleration RMS, and the overturning coefficient exhibit significant reductions from their pre-optimised values. Specifically, the mean square deviations decreased by 8.9%, 14.3%, and 51.3%, respectively. This shows that the fluctuation range of the objective functions is lower after applying MOFRO. In summary, the optimised results demonstrate enhanced robustness and reliability under dynamic operating conditions.

Table 5 Comparison of mean value and mean square deviation of optimisation objectives.

Objective functions	Original scheme		MOFRO	
	mean value	mean square deviation	mean value	mean square deviation
yaw acceleration RMS	1.18	0.045	1.06	0.041
lateral acceleration RMS	0.348	0.007	0.333	0.006
The overturning coefficient	0.242	0.039	0.175	0.019

Figure 6 illustrates a more direct observation of the robustness of optimisation objectives. It can be seen that the fluctuation degree of the objective function obtained after optimisation is "thinner", which indicates reduced sensitivity to random fluctuations in the design variables. The vehicle lateral stability is more robust and reliable.

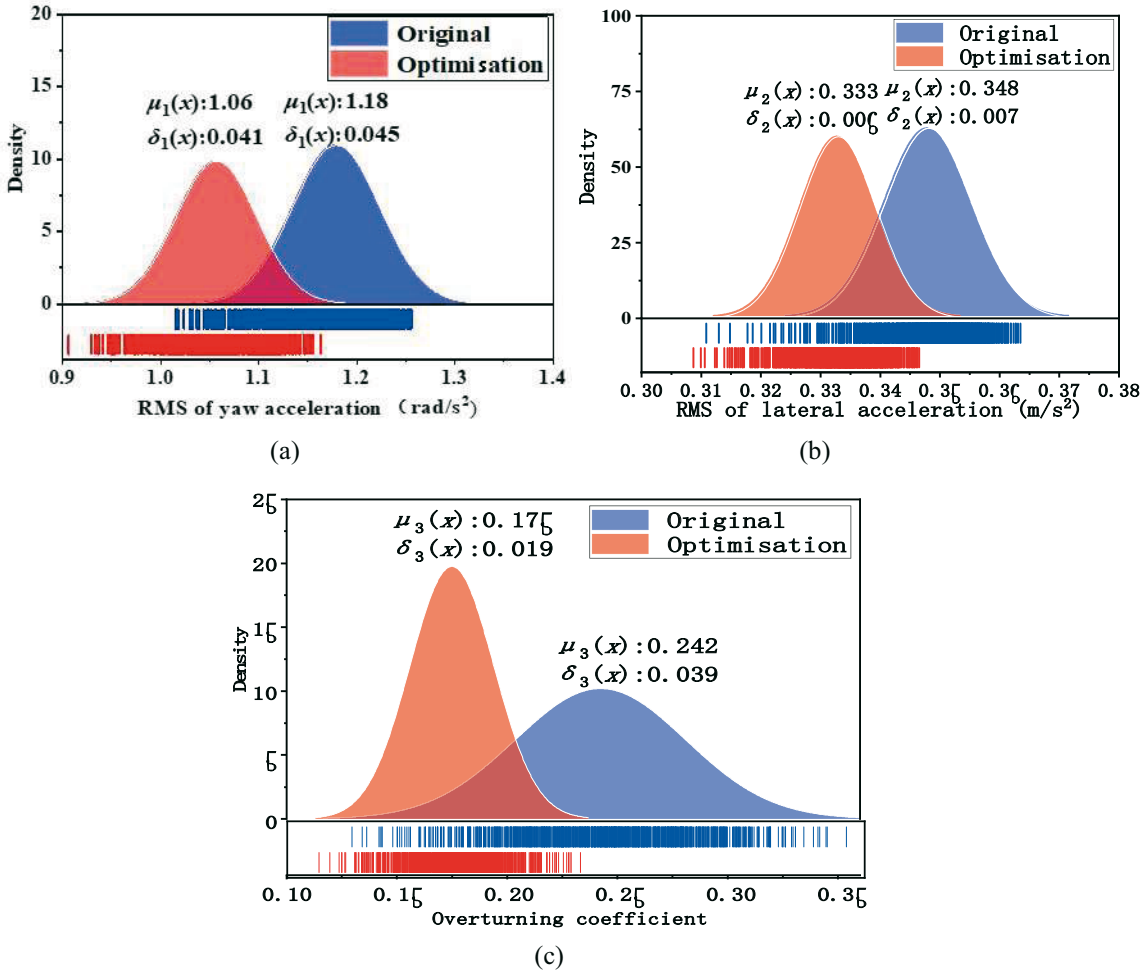

Fig. 6 Normal distribution diagram of optimisation objectives: (a) yaw acceleration RMS; (b) lateral acceleration RMS; (c) overturning coefficient.

4.2.2 Simulation analysis of the dynamic model

To verify the effect of lateral stability after the MOFRO of suspension parameters, optimised and original suspension parameters are inputted into the multi-body dynamics simulation model for a 30-second simulation. It can be observed from Figure 7 that the peak yaw acceleration, lateral acceleration, and overturning coefficient are reduced in the time domain. Their fluctuation amplitudes are reduced by 10.3%, 10.4%, and 25.6%, respectively. Figures 7(c) and 7(d) show that the lateral acceleration and yaw acceleration are reduced in the

frequency domain. This indicates that the vehicle lateral stability can be improved by using the MOFRO method.

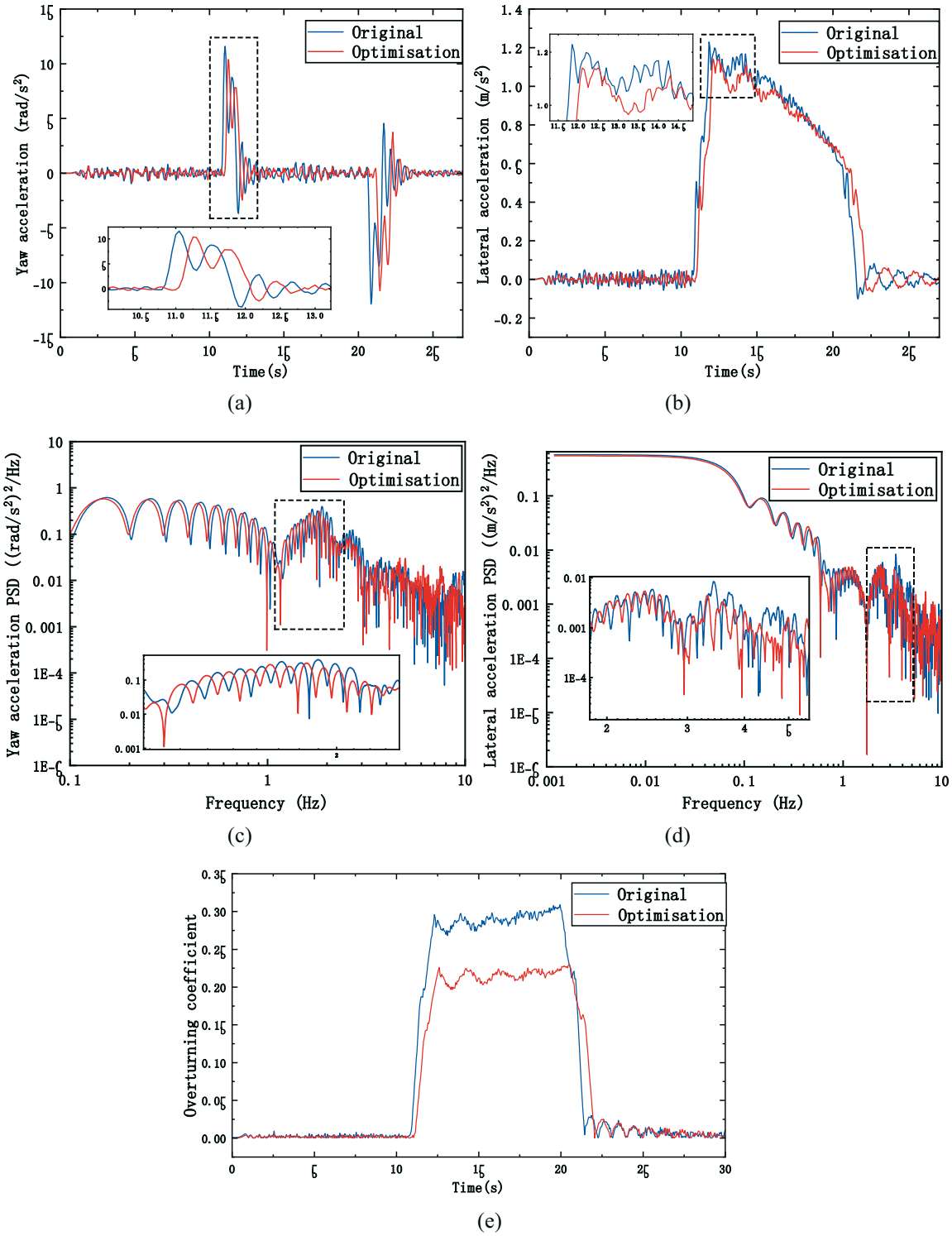

Fig. 7 Results of the comparison of optimisation objectives: (a) time domain plot of yaw acceleration; (b) time domain plot of lateral acceleration; (c) frequency domain plot of yaw acceleration; (d) frequency domain plot of lateral acceleration; (e) time domain plot of overturning coefficient.

Additionally, this study analyses the impact of the RMS value of yaw acceleration, the RMS value of lateral acceleration, and the maximum overturning coefficient under various speeds and loads. First of all, according to the suspension parameters of the original scheme

and the optimised suspension parameters in Table 5, the simulation model is utilised to simulate the optimisation objectives within the speeds from 20 km/h to 40 km/h. It can be seen in Figure 8 that the yaw acceleration RMS, the lateral acceleration RMS, and the maximum value of the overturning coefficient at the same speed are smaller than the original values. The fluctuation range of these optimisation objectives in the whole speed range is reduced by 11.35%, 3.44%, and 23.05%, respectively.

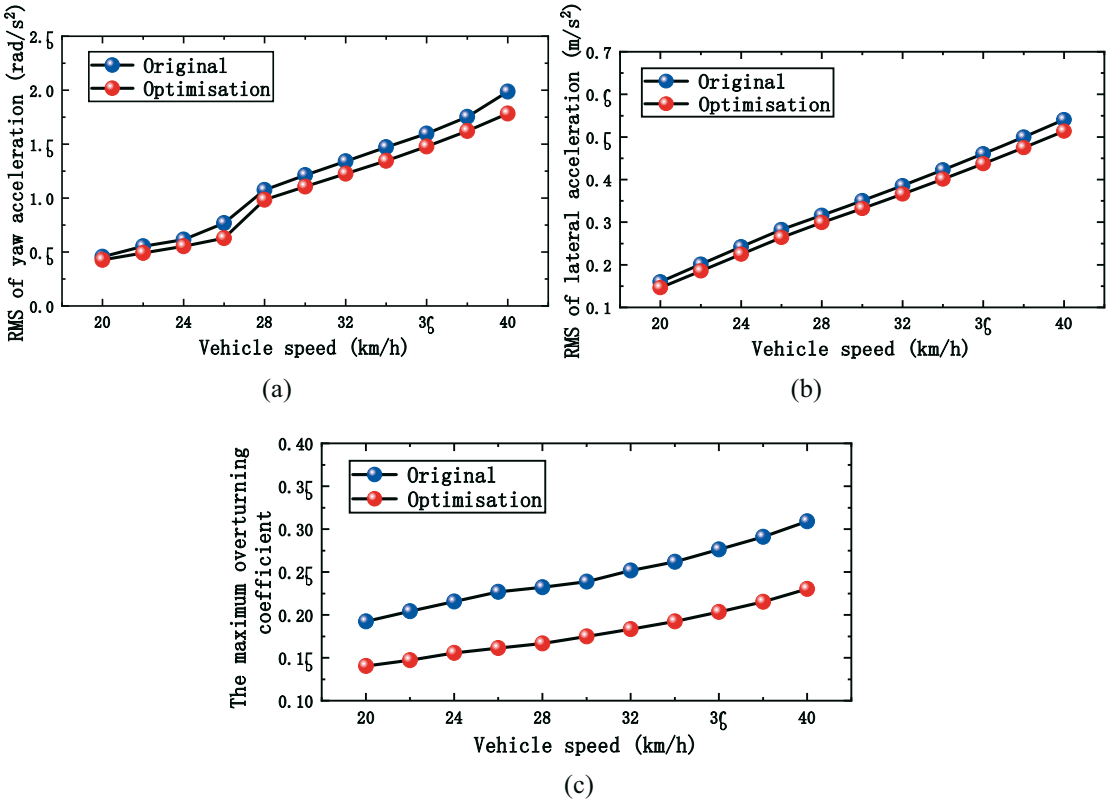

Fig. 8 Results of comparison for optimisation objectives under different vehicle speeds: (a) yaw acceleration RMS; (b) lateral acceleration RMS; (c) maximum overturning coefficient.

Similarly, the vehicle dynamics simulation model is used to simulate the optimisation objectives of the lateral stability under varying load conditions, ranging from no-load to half-load. The results of the optimisation objectives can be seen in Figure 9. Yaw acceleration RMS, lateral acceleration RMS, and the maximum value of the overturning coefficient under the same load are all reduced. The fluctuation range of the overturning coefficient in the whole load range is reduced by 30.3%.

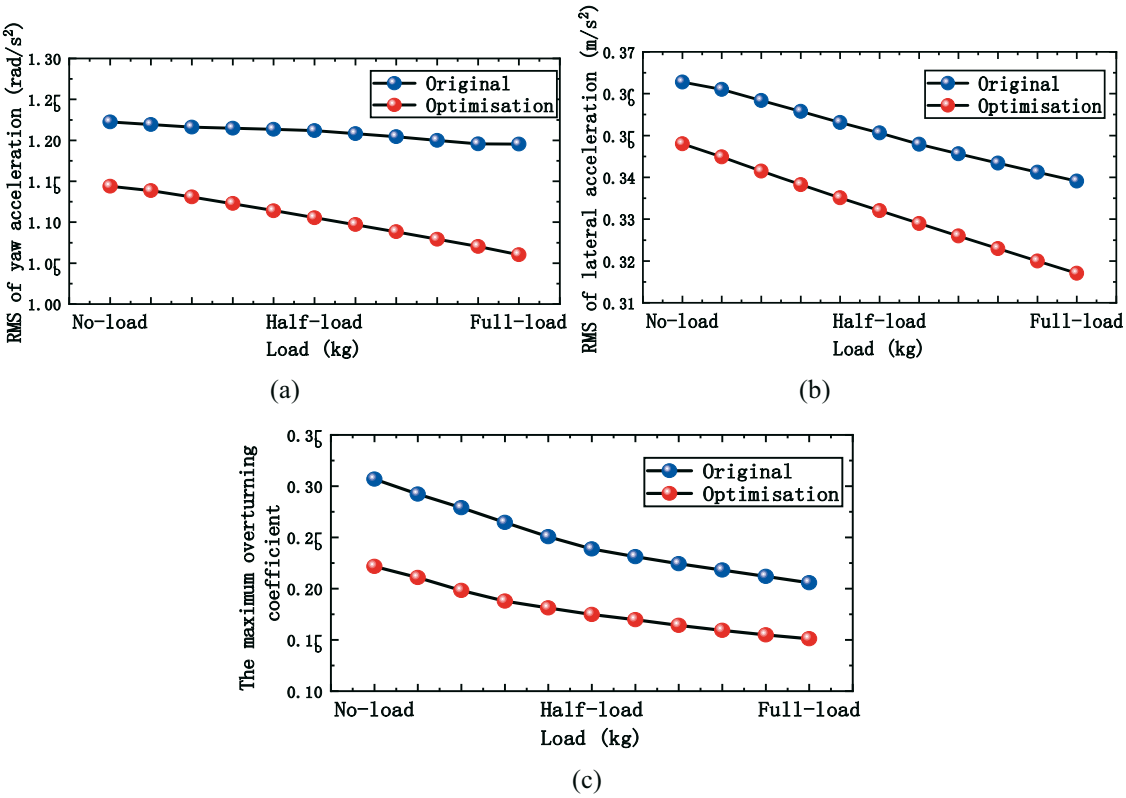

Fig. 9 Results of comparison of optimisation objectives under different loads: (a) yaw acceleration RMS; (b) lateral acceleration RMS; (c) maximum overturning coefficient.

The above analysis of Figures 8 and 9 demonstrates that the optimised combination of suspension parameters effectively enhances the vehicle lateral stability and reduces the fluctuation of dynamic performance.

5. Conclusions

This study employed an orthogonal experimental method to conduct a sensitivity analysis of the suspension parameters that affect the vehicle's lateral stability. An MOFRO approach was suggested to optimise the vehicle's suspension characteristics based on the findings of the analysis. In changeable situations, this optimisation increases lateral stability and offers highly resilient and reliable ideal solutions. The following are the primary conclusions:

(1) The drawbar length, the half distance of the vehicle, the vertical rigidity of the running wheel, the cornering rigidity of the running wheel, the vertical rigidity of the steering wheel, the vertical rigidity of the stabilising wheel, and the damping of the lateral damper have the most significant impact on the lateral stability of the vehicle, according to the sensitivity analysis of the suspension parameters for an STMV with single-axle bogies based on the orthogonal experimental method.

(2) For STMVs with single-axle bogies, a MOFRO model of the suspension parameters was built. Following iterative optimisation, the vehicle's overturning coefficient, lateral acceleration RMS, and yaw acceleration RMS were reduced by 8.3%, 5.4%, and 26.8%, respectively. The outcomes show that using the suggested strategy improves the vehicle's lateral stability.

(3) The vehicle was optimised and then its resilience was assessed using a Monte Carlo study. The findings show that, following optimisation, both the mean and the mean square deviation of the lateral stability indexes decreased. Specifically, the mean square deviation was reduced by 8.9%, 14.3%, and 51.3%, respectively. These reductions demonstrate how solid and dependable the vehicle's dynamic performance is.

(4) A comparison and analysis were conducted between the optimisation outcomes of the suspension parameters under the same conditions. The outcomes show that, in comparison to pre-optimisation, the optimisation goals for fluctuation range and lateral stability were reduced. This suggests a more potent ability to prevent interference. Furthermore, it offers a fresh method for designing rubber-type and monorail vehicles with stability optimisation, especially in the face of ambiguous variables like fluctuating conditions.

Disclosure Statement

No potential conflict of interest was reported by the authors.

Funding

This work was supported by the Intelligent Policing Key Laboratory of Sichuan Province (No. ZNJW2023KFQN005), the Sichuan Science and Technology Program (2024NSFSC2029) and the Luzhou Science and Technology Project (No. 2023JYJ066).

Abbreviations

STMV	straddle-type monorail vehicle
MOFRO	multi-objective fuzzy robustness optimisation
RMS	root mean square
NSGA-II	non-dominated Sorting Genetic Algorithm-II

REFERENCES

[1] Pulido D, Darido G, Munoz-Raskin R, et al. The urban rail development handbook. Washington: World Bank Publications, 2018. https://doi.org/10.1596/978-1-4648-1272-9

[2] He XH. Application and Prospect of Straddle Monorail Transit System in China. Urban Rail Transit 2015; 1: 26-34. https://doi.org/10.1007/s40864-015-0006-9

[3] Jiang YZ, Wu P, Zeng J, et al. Comparison of the curve negotiation properties of two different articulated monorail vehicles. Proceedings of the Institution of Mechanical Engineers Part F-Journal of Rail and Rapid Transit 2019; 233: 831-843. https://doi.org/10.1177/0954409718810946

[4] Wang HL and Zhu EY. Dynamic response analysis of monorail steel-concrete composite beam-train interaction system considering slip effect. Eng Struct 2018; 160: 257-269. https://doi.org/10.1016/j.engstruct.2018.01.037

[5] Xu XY, Lu HP, Hua X, et al. An Investigation on Dynamic Characteristics of the Straddle-Type Monorail System under Spatial Alignment. Machines 2022; 10: 724. https://doi.org/10.3390/machines10090724

[6] Cai CB, He QL, Zhu SY, et al. Dynamic interaction of suspension-type monorail vehicle and bridge: Numerical simulation and experiment. Mech Syst Sig Process 2019; 118: 388-407. https://doi.org/10.1016/j.ymssp.2018.08.062

[7] Naeimi M, Tatari M, Esmaeilzadeh A, et al. Dynamic interaction of the monorail-bridge system using a combined finite element multibody-based model. Proc Inst Mech Eng, Part K: J Multi-body Dyn 2015; 229: 132-151. https://doi.org/10.1177/1464419314551189

[8] Maciel GPR and Barbosa RS. Monorail vehicle model to study influence of tyre modelling on overall dynamics. Int J Heavy Veh Syst 2016; 23: 317-332. https://doi.org/10.1504/IJHVS.2016.079270

[9] Lee CH, Kawatani M, Kim CW, et al. Dynamic response of a monorail steel bridge under a moving train. J Sound Vib 2006; 294: 562-579. https://doi.org/10.1016/j.jsv.2005.12.028

[10] Lee CH, Kim CW, Kawatani M, et al. Dynamic response analysis of monorail bridges under moving trains and riding comfort of trains. Eng Struct 2005; 27: 1999-2013. https://doi.org/10.1016/j.engstruct.2005.06.014

[11] Zhou JC, Liu YH, Gao JJ, et al. Shimmy analysis of straddle-type monorail vehicle with single-axle bogies based on factor model. Veh Syst Dyn 2023: 22. https://doi.org/10.1080/00423114.2023.2211694

[12] Zhang X, Liu YQ, Yang SP, et al. Bifurcation analysis of the bogie system with time delay and the influence of parameters on the system. Veh Syst Dyn 2023: 17. https://doi.org/10.1080/00423114.2023.2252536

[13] Guo JY, Shi HL, Luo R, et al. Bifurcation analysis of a railway wheelset with nonlinear wheel-rail contact. Nonlinear Dyn 2021; 104: 989-1005. https://doi.org/10.1007/s11071-021-06373-8

[14] Mo W, Walker PD and Zhang N. Dynamic analysis and control for an electric vehicle with harpoon-shift synchronizer. Mech Mach Theory 2019; 133: 750-766. https://doi.org/10.1016/j.mechmachtheory.2018.11.018

[15] Jin TH, Liu ZM, Sun SS, et al. Theoretical and experimental investigation of a stiffness-controllable suspension for railway vehicles to avoid resonance. Int J Mech Sci 2020; 187: 105901. https://doi.org/10.1016/j.ijmecsci.2020.105901

[16] Yildiz AS and Sivrioglu S. Improving curving performance of a straddle type monorail vehicle by using semi-active devices. Int J Heavy Veh Syst 2021; 28: 385-408. https://doi.org/10.1504/Ijhvs.2021.117498

[17] Tu L, Du H, Dong M, et al. Semiactively Controllable Vehicle Seat Suspension System With Negative Stiffness Magnetic Spring. IEEE/ASME Trans Mechatron 2021; 26: 156-167. https://doi.org/10.1109/TMECH.2020.3006619

[18] Liu PF, Zheng MY, Ning DH, et al. Decoupling vibration control of a semi-active electrically interconnected suspension based on mechanical hardware-in-the-loop. Mech Syst Sig Process 2022; 166: 108455-108472. https://doi.org/10.1016/j.ymssp.2021.108455

[19] Deng W, Ni H, Liu Y, et al. An adaptive differential evolution algorithm based on belief space and generalized opposition-based learning for resource allocation. Appl Soft Comput 2022; 127: 109419. https://doi.org/10.1016/j.asoc.2022.109419

[20] Tang Q and Eberhard P. Cooperative Motion of Swarm Mobile Robots Based on Particle Swarm Optimization and Multibody System Dynamics. Mech Based Des Struct Mach 2011; 39: 179-193. https://doi.org/10.1080/15397734.2011.550855

[21] Gobbi M, Haque I, Papalambros PY, et al. Optimization and integration of ground vehicle systems. Veh Syst Dyn 2005; 43: 437-453. https://doi.org/10.1080/00423110500158841

[22] Gong D, Zhou JS and Sun WJ. Influence of under-chassis-suspended equipment on high-speed EMU trains and the design of suspension parameters. Proceedings of the Institution of Mechanical Engineers Part F-Journal of Rail and Rapid Transit 2016; 230: 1790-1802. https://doi.org/10.1177/0954409715614601

[23] Jiang YZ, Wu PB, Zeng J, et al. Multi-parameter and multi-objective optimisation of articulated monorail vehicle system dynamics using genetic algorithm. Veh Syst Dyn 2020; 58: 74-91. https://doi.org/10.1080/00423114.2019.1566557

[24] Yao Y, Li G, Wu G, et al. Suspension parameters optimum of high-speed train bogie for hunting stability robustness. Int J Rail Transp 2020; 8: 195-214. https://doi.org/10.1080/23248378.2019.1625824

[25] Wen XX, Huang LK, Du ZX, et al. Research on parameter optimization based on multi-body dynamics model of monorail vehicle aiming at reducing running wheel wear. Proc Inst Mech Eng, Part K: J Multi-body Dyn 2022; 236: 588-601. https://doi.org/10.1177/14644193221119331

[26] Wu HX, Du ZX, Yang Z, et al. Coordination and matching of tire system of new straddle-type rapid transit vehicle. Veh Syst Dyn 2023; 61: 573-588. https://doi.org/10.1080/00423114.2022.2051568

[27] Li YL, She L, Wen LF, et al. Sensitivity analysis of drilling parameters in rock rotary drilling process based on orthogonal test method. Eng Geol 2020; 270: 105576. https://doi.org/10.1016/j.enggeo.2020.105576

[28] Sun GY, Li GY, Zhou SW, et al. Crashworthiness design of vehicle by using multiobjective robust optimization. Struct Multidiscip Optim 2011; 44: 99-110. https://doi.org/10.1007/s00158-010-0601-z

[29] Tey JY, Ramli R and Abdullah AS. A new multi-objective optimization method for full-vehicle suspension systems. Proc Inst Mech Eng, Part D: J Automob Eng 2016; 230: 1443-1458. https://doi.org/10.1177/0954407015611522

[30] Hassine R, Karray F, Alimi AM, et al. Approximation properties of piece-wise parabolic functions fuzzy logic systems. Fuzzy Sets Syst 2006; 157: 501-515. https://doi.org/10.1016/j.fss.2005.07.004

[31] Pan YJ, Zhang C, Yin BH, et al. Fuzzy set based multi-objective optimization for eight-rod mechanism via sensitivity analysis. Proc Inst Mech Eng, Part D: J Automob Eng 2019; 233: 333-343. https://doi.org/10.1177/0954407017743358

[32] Kaur D, Mukherjee S and Basu K. Solution of a Multi-Objective and Multi-Index Real-Life Transportation Problem Using Different Fuzzy Membership Functions. J Optim Theory Appl 2015; 164: 666-678. https://doi.org/10.1007/s10957-014-0579-6

[33] Zhou JC, Zhang BH, Yin JL, et al. Sensitivity-based, space rod system multi-objective design of straddle-type monorail vehicle with single-axle bogies. Mech Based Des Struct Mach 2022. https://doi.org/10.1080/15397734.2022.2120496

[34] Mechanical vibration and shock — Evaluation of human exposure to whole-body vibration — Part 1: General requirements, https://www.iso.org/standard/7612.html

[35] Lin TR. A comparative study between smaller-the-better and normal-the-best quality characteristics when lapping ceramic blocks. Int J Adv Manuf Technol 2006; 31: 155-163. https://doi.org/10.1007/s00170-005-0179-6

Submitted: 09.7.2024

Accepted: 02.7.2025

Junchao Zhou[1,2]
Ao Chen[1]
Yihan Liu[1]
Jianjie Gao[3*]
Jie Zhang[4]
Haiping Du[5]
Fei Tang[6]
[1] School of Mechanical Engineering, Sichuan University of Science and Engineering, Zigong, PR China
[2] Chengdu-Chongqing Economic Circle (Luzhou) Advanced Technology Research Institute, Luzhou, PR China
[3] Intelligent Policing Key Laboratory of Sichuan Province, Sichuan Police College, Luzhou, PR China
[4] College of Automotive and Mechanical Engineering, Changsha University of Science and Technology, Changsha, PR China
[5] School of Electrical, Computer & Telecommunications Engineering, University of Wollongong, New South Wales 2522, Australia
[6] Cheng Du Connect Rail Transit Equipment Co., Ltd, Chengdu, PR China
[*]Corresponding author: jianjiecq@163.com